刘佳琦,臧延青. 生物信息学和网络药理学证实红桑葚水提物能改善糖尿病作用 [J]. 食品工业科技, 2026, 47(8): 456−469. doi: 10.13386/j.issn1002-0306.2025040312

LIU Jiaqi, ZANG Yanqing. Bioinformatics and Network Pharmacology Confirmed that Red Mulberry Water Extract Can Improve Diabetes[J]. Science and Technology of Food Industry, 2026, 47(8): 456−469. (in Chinese with English abstract). doi: 10.13386/j.issn1002-0306.2025040312

·营养与保健·

生物信息学和网络药理学证实红桑葚水提物能改善糖尿病作用

刘佳琦[1],臧延青[1,2,*]

(1.黑龙江八一农垦大学食品学院,黑龙江大庆 163000;
2.国家杂粮工程技术中心,黑龙江大庆 163000)

摘　要:2 型糖尿病（Type 2 diabetes mellitus，T2DM）是最常见的糖尿病类型。本研究采用网络药理学、代谢组学和实验验证相结合的整合策略，阐明了红桑葚水提物（red mulberry water extract，RMW）治疗 T2DM 的作用机制。系统分析鉴定出 6 种生物活性成分，其中 4 种关键成分 (花青素、槲皮素、桑色素和 β-胡萝卜素）与糖尿病相关靶点具有显著相互作用。网络药理学分析显示，这些成分调控 AMPK（P=2.3×10^{-5}）、PI3K-Akt（P=1.8×10^{-4}）和 PPAR（P=3.1×10^{-3}）等关键通路。在糖尿病小鼠中，治疗显著改善了血糖控制（空腹血糖降低 32.5%，P<0.01)、血脂谱（TG 降低 36.7%，P<0.05）、抗氧化活性（SOD 增加 2.1 倍，P<0.05）和炎症反应（TNF-α 降低 42%，P<0.05）。代谢组学分析进一步证实了儿茶酚胺和脂质代谢通路的改变。这些发现共同证明了桑葚通过协同调节葡萄糖代谢、脂质稳态、氧化应激和炎症反应，具有多靶点治疗糖尿病的潜力。

关键词:桑葚,2 型糖尿病,网络药理学,生物活性成分,胰岛素抵抗,PPAR 信号通路,氧化应激
中图分类号:TS255.1　　**文献标识码:**A　　**文章编号:**1002−0306(2026)08−0456−14
DOI: 10.13386/j.issn1002-0306.2025040312
本文网刊:

Bioinformatics and Network Pharmacology Confirmed that Red Mulberry Water Extract Can Improve Diabetes

LIU Jiaqi[1], ZANG Yanqing[1,2,*]

(1.College of Food Science, Heilongjiang Bayi Agricultural University, Daqing 163000, China;
2.National Coarse Cereals Engineering Research Center, Daqing 163000, China)

Abstract: Type 2 diabetes mellitus (T2DM) was identified as the most prevalent form of diabetes. This study employed an integrated strategy combining network pharmacology, metabolomics, and experimental validation to elucidate the therapeutic mechanisms of red mulberry water extract (RMW) in T2DM. Systematic analysis identified six bioactive constituents, with four key components (cyanidin, quercetin, morin, and β-carotene) demonstrating significant interactions with diabetes-related targets. Network pharmacology revealed these compounds modulate critical pathways including AMPK (P=2.3×10^{-5}), PI3K-Akt (P=1.8×10^{-4}), and PPAR signaling (P=3.1×10^{-3}). In diabetic mice, treatment significantly improved glycemic control (32.5% reduction in fasting glucose, P<0.01), lipid profiles (36.7% lower TG, P<0.05), antioxidant activity (2.1-fold increased SOD, P<0.05), and inflammation (42% reduced TNF-α, P<0.05). Metabolomic analysis further confirmed alterations in catecholamine and lipid metabolism pathways. These findings collectively demonstrate mulberry's multi-target therapeutic potential through synergistic regulation of glucose metabolism, lipid homeostasis, oxidative stress, and inflammatory responses in diabetes.

Key words: mulberry; type 2 diabetes mellitus (T2DM); network pharmacology; bioactive compounds; insulin resistance; PPAR signaling; oxidative stress

收稿日期: 2025−04−25

作者简介: 刘佳琦（1998−）,女,硕士研究生,研究方向:食品营养与质量安全,E-mail: 974798142@qq.com。

*** 通信作者:** 臧延青（1974−）,女,博士,教授,研究方向:食品营养与质量安全,E-mail: byndzangyanqing@163.com。

Diabetes mellitus is a chronic metabolic disorder characterized by persistent hyperglycemia resulting from defects in insulin secretion, insulin action, or both. It is a major global health concern with significant implications for individual morbidity and mortality[1]. Type 2 diabetes mellitus (T2DM), the most prevalent form, accounts for approximately 90%~95% of all cases and is increasingly prevalent due to aging populations, sedentary lifestyles, and dietary changes[2]. As the disease burden intensifies, researchers are exploring integrated treatment strategies that combine natural products with modern biomedical technologies to enhance therapeutic efficacy and minimize side effects[3].

Morus alba L. (mulberry fruit) has been selected as an ideal material for diabetes intervention research due to its longstanding medicinal tradition and well-defined bioactive constituent profile. As a resource of medicinal food homology in traditional Chinese medicine, it is rich in characteristic functional components: 1-Deoxynojirimycin (1-DNJ) serves as a potent dual inhibitor of both α-glucosidase and sucrase, effectively delaying intestinal carbohydrate hydrolysis/digestion and subsequent glucose absorption[4], mulberry polysaccharides ameliorate insulin resistance by modulating gut microbiota composition and suppressing the TLR4/MyD88/NF-κB inflammatory pathway[5], while cyanidin-3-glucoside (C3G) derived from *Morus alba* L. demonstrates β-cell protective capacity through novel mechanisms, particularly by attenuating extracellular signal-regulated kinase (ERK) and p38 phosphorylation cascades while regulating intrinsic apoptosis pathway components to mitigate oxidative stress-induced pancreatic β-cell dysfunction[6]. The mulberry extract achieves multi-pathway glucose regulation through coordinated inhibition of carbohydrate hydrolases, potentiation of insulin signaling pathways, and improvement of islet cell function, with its core active constituents demonstrating significant glucose-lowering efficacy in diabetic models[7−9]. Given its traditional application basis and multi-target mechanisms, mulberry represents a promising candidate for developing natural antidiabetic therapeutics.

Network pharmacology has emerged as a powerful tool to investigate the complex interactions between multiple compounds and targets, especially in traditional Chinese medicine. By integrating systems biology, bioinformatics, and pharmacology, network pharmacology enables the systematic elucidation of drug–target–disease relationships[10−11]. For example, Yang et al[12] utilized network pharmacology and molecular docking integrated experiments to verify that *Gynostemma pentaphyllum* could improve insulin resistance and thereby regulate T2DM by modulating the IRS1/PI3K/Akt signaling pathway. Deng et al[13] found that the food and medicine homology (FMH) complex could modulate lipid metabolism and inflammatory pathways to improve metabolic-associated fatty liver disease. Wang et al[14] found that the ethanol extract of mulberry leaves can alleviate T2DM by regulating multiple target proteins and pathways involved in its pathogenesis. Despite its advantages, the predictive outcomes of network pharmacology must be experimentally validated to ensure translational relevance[15−16]. Thus, combining network pharmacology with *in vivo* studies provides a multidimensional framework for uncovering the mechanisms of natural compounds in T2DM therapy and guiding the development of effective treatment strategies.

1 Materials and methods

1.1 Materials and instruments

Red Mulberry (*Morus alba* L.) water extract (RMW) Shaanxi Xintianyu Biotechnology Co., Ltd. The extract was stored in a cool, dry place protected from light until use; Male C57BL/6 mice (6-week-old, body weight 20±2 g, License No.: SCXK (Liao) 2020-0001) Liaoning Changsheng Biotechnology Co., Ltd.; All experimental operations complied with the national guidelines for laboratory animal management and use (laboratory animal ethics number: SPXY2024002). Mice were housed in controlled environments with stable temperature and humidity, ensuring a hygienic condition. They were subjected to a 12-hour light/dark cycle and provided with ad libitum access to food and water for an acclimatization period of 7 d; Standard maintenance diet (Grade A) Shenyang Maohua Biotechnology Co. Ltd. Biochemical kits for total cholesterol (TC), triglycerides (TG), total protein (TP), high-density lipoprotein cholesterol (HDL-C), low-density lipoprotein cholesterol (LDL-C) and alanine aminotransferase (ALT) Nanjing Jiancheng Bioengineering Institute; Kits for glutathione (GSH), nitric oxide (NO), glutathione peroxidase (GSH-Px), catalase (CAT), superoxide dismutase (SOD), malondialdehyde (MDA), insulin (INS), glycated hemoglobin (HbA1c), interleukin-1β (IL-1β) and tumor necrosis factor-α (TNF-α) Suzhou Grace Biotechnology Co.,

Ltd.; All other chemicals were of analytical grade.

PerkinElmer VICTOR Nivo microplate reader PerkinElmer Management (Shanghai) Co., Ltd.; E-2000A rotary evaporator Zhengzhou Yarong Instrument Co., Ltd.; DELTA 320 precision pH meter Mettler-Toledo Instruments (Shanghai) Co., Ltd.; Agilent 1200 HPLC system Agilent Technologies, USA; UV1800 UV-Vis spectrophotometer Shimadzu Corporation, Japan; glucometer Accu-Chek Performa, Roche.

1.2 Experimental methods

1.2.1 Network pharmacology analysis Based on the previous studies, the main bioactive components of *Morus alba* L. were screened using the Traditional Chinese Medicine Systems Pharmacology Database (TCMSP, http://tcmspw.com/) with the criteria of oral bioavailability (OB)≥30% and drug-likeness (DL)≥0.18[17−19]. Chemical similarity analysis and pharmacophore models were then applied to predict the potential targets of these compounds. The obtained targets were standardized via the UniProt database, and diabetes-related disease targets were retrieved from the DisGeNET database (https://www.disgenet.org/) using a relevance score threshold of ≥0.3.

1.2.2 Chemical composition analysis The quantification of total polyphenols adhered to the group standard set forth by the Anhui Food Industry Association (T/AHFIA). The standard curve was established using gallic acid as a reference (concentration range: 10~60 μg/mL), with the equation: y=0.0109x+0.0277 (R^2=0.9990). The quantification of total flavone content was executed through spectrophotometric analysis[20]. Catechin was used as the standard (0~200 μg/mL), and the calibration curve was fitted to the equation: y=0.0006x+0.0062 (R^2=0.9882). The polysaccharide content was determined by the phenol-sulfuric acid method[20]. Glucose was used as the standard (0~100 μg/mL), and the curve equation was y=0.0074x+0.0065 (R^2=0.9992). The measurement of total anthocyanin content was accomplished using the pH differential method[21].

1.2.3 Antioxidant activity determination The methods for determining DPPH, $ABTS^+$, and hydroxyl radical scavenging capacities were adapted based on the procedures described in references[22−24], with modifications made in accordance with standard protocols commonly used in antioxidant activity assay manuals.

1.2.3.1 DPPH radical scavenging assay Sample solutions were mixed with 50 μg/mL DPPH ethanol solution and incubated in the dark for 30 min. Absorbance was measured at 517 nm. The radical scavenging rate was calculated as:

$$\text{DPPH radical scavenging activity}(\%) = \left(1-\frac{A_s-A_c}{A_b}\right)\times 100$$

where A_s=absorbance of sample+DPPH; A_c=absorbance of sample+ethanol (control); A_b=absorbance of DPPH+solvent (blank).

1.2.3.2 $ABTS^+$ radical scavenging assay Sample solutions were reacted with ABTS working solution (adjusted to absorbance 0.70±0.02 at 734 nm), incubated for 5 min in the dark, and absorbance measured at 734 nm. Scavenging rate was calculated as:

$$ABTS^+\text{radical scavenging activity}(\%) = \left(1-\frac{A_s}{A_b}\right)\times 100$$

where A_s=absorbance of sample+ABTS; A_b=absorbance of ABTS+solvent (blank).

1.2.3.3 Hydroxyl radical scavenging assay Equal volumes of $FeSO_4$, salicylic acid solution, and sample were mixed (1∶1∶1), followed by equal volume of H_2O_2. Mixtures were incubated at 37 ℃ for 1 h, and absorbance measured. Scavenging activity was calculated by:

$$\text{Hydroxyl scavenging activity}(\%) = \left[1-\frac{(A_1-A_2)}{A_0}\right]\times 100$$

where A_0=absorbance of blank (70% ethanol replacing sample); A_1=absorbance of test sample; A_2=absorbance of control (deionized water replacing salicylic acid).

1.2.4 Identification and analysis of compounds in RMW The RMW were subjected to analysis utilizing an Ultimate 3000 UPLC/Q-Exactive orbitrap mass spectrometer. The chromatographic parameters were optimized based on previous studies[25−27], with slight modifications to suit the specific requirements of analyzing RMW. The parameters were as follows: a Kromasil C_{18} column (250 mm×4.6 mm inner diameter) was employed at a column temperature of 50 ℃, with an injection volume of 30 μL and a detection wavelength set at 525 nm, operating at a flow rate of 1 mL per minute. The mobile phase was composed of solvent A, a 2% (v/v) aqueous formic acid solution, and solvent B, acetonitrile containing

2% (v/v) formic acid. A gradient elution program was initiated at 6% B, increasing to 10% B within the initial 2 min, then to 25% B by the 8th minute, where it was held constant until the 9th minute. Subsequently, the gradient was adjusted to 40% B by the 15th minute, 60% B by the 17th minute, and finally to 100% B by the 20th minute, which was sustained for an additional 5 min. Mass spectrometry was conducted under conditions optimized for flavonoids in positive ion mode and for non-flavonoid compounds in negative ion mode, with a mass range spanning from 100 to 1500 m/z. The nebulizer was operated at a pressure of 30 psi, the desolvation gas flow rate was set at 10 L/min, and the desolvation temperature was maintained at 325 ℃. Each sample was processed in triplicate for analytical consistency.

1.2.5 Animal grouping and feeding Protocol All experimental procedures were approved by the Institutional Animal Care and Use Committee (Approval No. SPXY2024002) and conducted in accordance with the National Institutes of Health Guide for the Care and Use of Laboratory Animals. Six-week-old male C57BL/6J mice were maintained under standard laboratory conditions (22±2 ℃, 50%~60% relative humidity) with a 12-hour light/dark cycle. Following one week of acclimatization, the animals were then randomly divided into four groups based on previously described methods[28−29]: Normal diet control group (ND) receiving standard chow, HFD-induced model group (HD), metformin-treated group (MET) administered 200 mg/kg metformin, and RMW-treated group (RMW) administered 800 mg/kg RMW. All treatment groups were maintained on HFD throughout the 8-week experimental period.

All animals had free access to food and water ad libitum throughout the experimental period. Body weights were recorded weekly using a precision electronic balance (±0.1 g). The high-fat diet feeding protocol successfully induced T2DM, as evidenced by fasting blood glucose levels≥11.1 mmol/L in the HD group[30]. Treatment groups received daily oral administration of test compounds, while control groups were provided with equivalent volumes of drinking water. All experimental procedures were performed in compliance with institutional animal care guidelines.

1.2.6 Measurement and analytical methods

1.2.6.1 Glucose metabolism assessment Weekly fasting blood glucose (FBG) levels were determined after 10-hour fasting through tail vein blood sampling using a glucometer (Accu-Chek Performa, Roche). Serum INS and HbA1c levels were measured using commercial ELISA kits following the manufacturer's protocols. The oral glucose tolerance test (OGTT) was performed at week 7 after grouping, with mice fasted for 10 hours prior to receiving an oral glucose load (2 g/kg body weight). Blood glucose concentrations were measured at 0, 30, 60, 90 and 120 minutes post-administration via tail vein sampling, and the area under the curve (AUC) was calculated to assess glucose tolerance.

1.2.6.2 Hepatic oxidative stress evaluation For evaluation of hepatic oxidative stress, liver tissues were homogenized in ice-cold physiological saline (1∶9, w/v) and centrifuged (3500 r/min, 10 min, 4 ℃). The resulting supernatant was used to measure oxidative stress markers including GSH, GSH-Px, SOD, CAT, NO, and MDA using commercial kits.

1.2.6.3 Inflammatory cytokine and liver function assessment Serum levels of inflammatory cytokines (TNF-α and IL-1β) were quantified using ELISA kits following the manufacturer's protocols. ALT activity was measured as an indicator of liver function using commercial assay kits.

1.2.6.4 Tissue collection and processing At study termination, blood samples were collected via cardiac puncture and processed for serum separation (3500 r/min, 10 min, 4 ℃). Major organs (heart, liver, kidneys, spleen, lungs, and pancreas) and adipose tissues (epididymal, perirenal, mesenteric white adipose tissue (WAT) and brown adipose tissue (BAT)) were excised, weighed, and stored at −80 ℃ for subsequent analyses. Organ and fat indices were calculated as the ratio of tissue weight to final body weight. The organ index (Viscera index, %) and fat index (Fat index, %) were calculated as follows:

$$\text{Organ index}(\%) = \frac{O_w}{O_b} \times 100$$

$$\text{Fat index}(\%) = \frac{F_w}{B_w} \times 100$$

Where O_w=Organ weight (g); O_b=Body weight (g); B_w=Body weight at sacrifice(g); F_w=Fat tissue weight(g).

1.3 Statistical analysis

All experimental data were presented as the mean value±standard deviation (SD). The statistical evaluation was conducted via one-way analysis of

variance (ANOVA), followed by post-hoc analysis using SPSS software (SPSS Inc., Chicago, IL, USA). Inter-group differences were considered statistically significant at the $P<0.05$ threshold.

2 Results and discussion

2.1 Acquisition of effective components and targets of mulberry

A total of ninety-one constituents were characterized within the TCMSP. Through the application of OB and DL criteria, six principal bioactive components were selected for further investigation. These compounds were then standardized and converted using additional databases to predict their potential targets. It is noteworthy that two of these constituents did not align with the identified target profiles, possibly due to limitations in current database annotations or inconsistencies in compound-target mapping during the data integration process. Therefore, the active ingredients that were further analyzed were cyanin, quercetin, morin and beta-carotene (Table 1). After all, the targets were integrated and the repeats were removed, 158 targets related to active components of mulberry were obtained.

Table 1 Bioactive ingredients of mulberry

Mol ID	Molecule Name	MW	OB(%)	DL	Targets
MOL006209	cyanin	411.66	47.42	0.76	2
MOL000098	quercetin	302.25	46.43	0.28	154
MOL000737	morin	302.25	46.23	0.27	17
MOL010300	dIDP	446.74	41.08	0.57	N/A
MOL002773	beta-carotene	536.96	37.18	0.58	22
MOL002372	(6Z,10E,14E,18E)-2,6,10,15,19,23-hexamethyltetracosa-2,6,10,14,18,22-hexaene	410.8	33.55	0.42	N/A

Note: "N/A"=Not available; No validated target information retrieved after database standardization.

2.2 Acquisition of disease targets for diabetes

Fifty-eight diabetes-related gene targets were selected from data from multiple database platforms. A total of 247 gene-disease associations were retrieved from the DisGeNET database, 1189 were sourced from the GeneCards database, 75 were extracted from the OMIM database, and 167 were identified from the Therapeutic Target Database (TTD). Three and all cross-genes in the database were selected, and 58 diabetes related gene targets were obtained after removing duplicate values. The enrichment analysis of the intersecting genes mentioned above was conducted using the Metascape software platform, yielding pathways and processes (Table 2). The initial 14 significant enrichment terms were selected for further consideration.

Table 2 Diabetes disease gene and pathway enrichment bar chart

GO	Description	Count	lg(*P*)	lg(q)
hsa04950	Maturity onset diabetes of the young	10	−20.82	−18.27
hsa04930	Type II diabetes mellitus	11	−20.23	−17.98
hsa05323	Rheumatoid arthritis	11	−16.60	−14.53
hsa04932	Non-alcoholic fatty liver disease	12	−15.82	−13.87
hsa04152	AMPK signaling pathway	10	−13.50	−11.73
hsa04911	Insulin secretion	9	−13.13	−11.43
hsa04066	HIF-1 signaling pathway	8	−10.45	−8.98
hsa04148	Efferocytosis	5	−4.90	−4.02
hsa05410	Hypertrophic cardiomyopathy	4	−4.44	−3.59
hsa00500	Starch and sucrose metabolism	3	−4.34	−3.52
hsa03320	PPAR signaling pathway	3	−3.39	−2.71
hsa04080	Neuroactive ligand-receptor interaction	5	−3.16	−2.51
hsa05215	Prostate cancer	3	−3.06	−2.43
hsa05207	Chemical carcinogenesis - receptor activation	3	−2.10	−1.55

2.3 Cross analysis of target genes related to mulberry and diabetes

A total of 12 cross-target genes were obtained from 158 mulberry target genes and 58 diabetes target genes screened above. The 12 crossing genes were VEGFA, TNF, TGFB1, SLC2A4, PPARG, PPARA, PIK3CG, MGAM, INSR, IL6, IL1B, and IL1A. (Figure 1A).

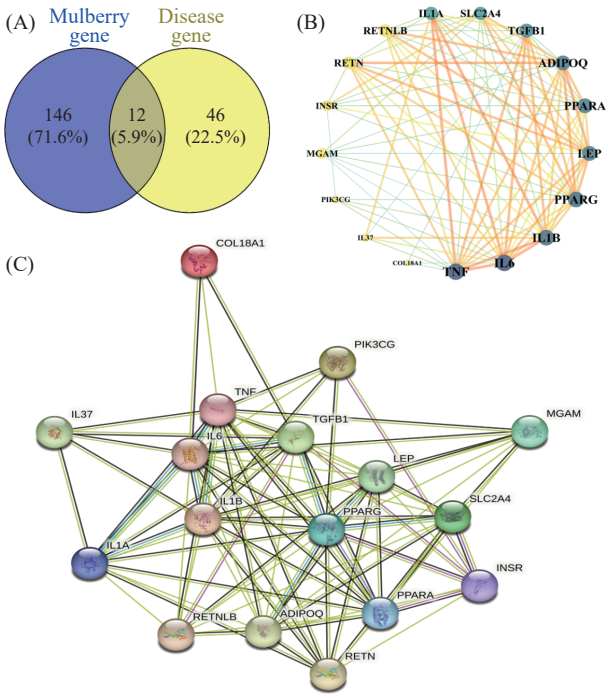


Fig.1 Overlapping targets and protein interactions between mulberry components and diabetes

Notes: (A)Venn diagram of active ingredient target genes of mulberry and diabetic disease target genes; (B) PPI interaction network generated by the STRING database; (C) PPI interaction network generated by Cytoscape software.

To further explore the interactions among these shared targets, a protein–protein interaction (PPI)

network was constructed. Figure 1B presented the interaction network generated via the STRING database. Subsequently, the data were imported into Cytoscape for visualization and topological analysis (Figure 1C). The network analysis yielded 12 known proteins and predicted 5 additional functional proteins through interaction enrichment, resulting in a total of 17 nodes.

2.4 Development of an integrated disease-pathway-target-component-drug interaction framework

Visualize the sample using Cytoscape3.7.2 and build networks to further identify key active ingredients and targets for diabetes in mulberry (Figure 2). As depicted in Figure 2(A), the network comprised 189 nodes and 203 edges. Nodes represent mulberry, active ingredients, diseases, pathways, and target genes, while edges denote the interactions among them. The degree of interaction values was used to determine the importance of nodes in each given network. Figure 2(B) illustrated a network analysis identifying the 20 most highly connected target nodes. The findings indicated that quercetin is a predominant bioactive constituent within the mulberry. A correlation analysis revealed that pathways such as the Diabetes and Longevity regulating pathway, Hematopoietic cell lineage, MAPK signaling pathway, PI3K-Akt signaling pathway, FoxO signaling pathway, and HIF-1 signaling pathway exhibit significant associations. It is evident from the visual representation that mulberry exerted its regulatory effects primarily through quercetin, which modulates key genes such as INSR, IL1A, and IL6. These pathways, in turn, were implicated in the modulation of diabetes.

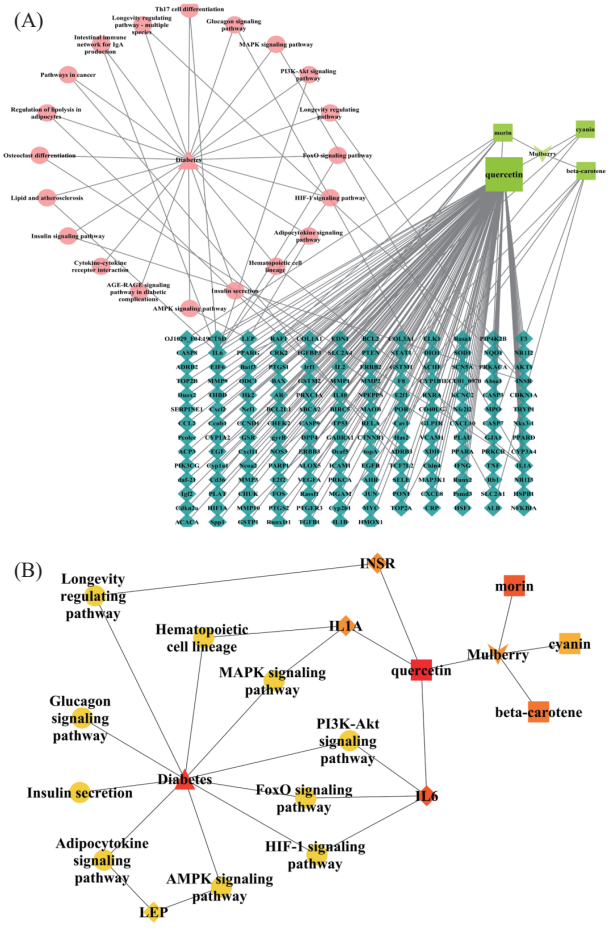


Fig.2　Targeted pathway network diagram

Notes: (A)Disease-pathway-target-component-drug network; (B) The 20 targets with the highest degree selected by the network analysis tool.

2.5 GO enrichment analysis and KEGG pathway annotation

Gene ontology (GO) enrichment analysis was conducted to identify pivotal biological processes, cellular components, and molecular functions associated with the mulberry's regulatory effects on diabetes mellitus, as illustrated in Figure 3(A). The analysis uncovered 162 significant biological processes (BP), 8 cellular components (CC), and 8 enriched molecular functions (MF). The results indicated that mulberry is predominantly involved in the positive modulation of MAP kinase activity, gene expression, interleukin-6 production, and inflammatory responses, among other biological processes. These processes were mediated through various cellular components, including the cell surface, secretory vesicles, and the extracellular space. Furthermore, mulberry was suggested to perform molecular functions such as cytokine activity, identical protein binding, growth factor activity, and general protein binding.

The kyoto encyclopedia of genes and genomes (KEGG) pathway revealed that mulberry primarily influenced metabolic and inflammatory pathways relevant to diabetes regulation. Key pathways included: a. insulin resistance, b. AGE-RAGE signaling in diabetic complications, c. FoxO signaling pathway, and d. cytokine-cytokine receptor interaction. Furthermore, mulberry also modulated pathways associated with diabetes-related comorbidities, including non-alcoholic fatty liver disease and alcoholic liver disease. The involvement of inflammatory pathways (MAPK signaling, osteoclast differentiation) further suggested mulberry's potential in ameliorating diabetes-associated low-grade inflammation (Figure 3(B)).

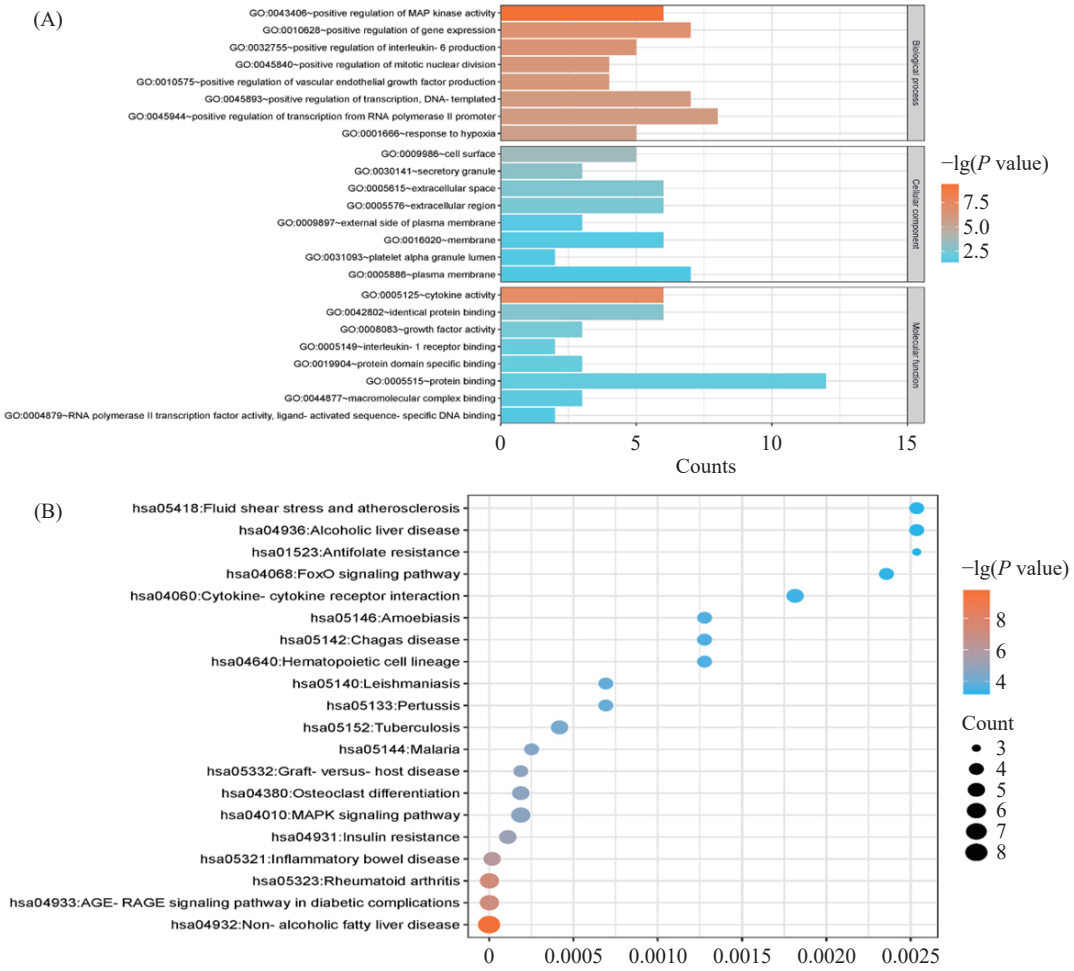


Fig.3 GO enrichment analysis histogram and KEGG channel annotated bubble map

Note: (A) GO enrichment analysis; (B) KEGG pathway analysis.

2.6 Main component content and antioxidant capacity of extracts of RMW

The high levels of bioactive compounds in mulberry, including polyphenols, flavonoids, polysaccharides, and anthocyanins[31]. In this study, the total polyphenol content was 29.10±0.58 mg GAE·g^{-1} DM (where GAE stands for gallic acid equivalents), the total flavonoid content was 10.35±0.01 mg CE·g^{-1} DM (where CE stands for catechin equivalents), the total polysaccharide content was determined to be 88.67±2.01 mg/g, and the total anthocyanin content was 0.83±0.18 mg/g. Suriyaprom et al.[32] reported a total polyphenol content of approximately 23.5 mg GAE/g and a total flavonoid content of 1.3 mg CE/g in the aqueous extract of white mulberry fruit. These values were lower than those obtained in this study, the findings suggested that RMW contains a richer concentration of both polyphenols and flavonoids. Additionally, previous study suggested that the high total polysaccharide content is particularly noteworthy, as polysaccharides are known to possess a wide range of biological activities, including antioxidant, immunomodulatory, and anti-inflammatory effects[33].

To investigate the antioxidant capacity of RMW, the study used radical scavenging assays. The results were showed in Table 3. Specifically, at a concentration of 1.0 mg/mL, the scavenging efficiencies for DPPH, ABTS^{+}, and hydroxyl radicals were 36.70%±2.09%, 66.27%±1.83%, and 12.22%±1.21%, respectively. At 2.0 mg/mL, these values increased to 68.09%±0.68%, 97.41%±0.01%, and 23.98%±0.56%, respectively. These findings indicated a clear enhancement in antioxidant activity with increasing RMW concentration, particularly in the ABTS assay. The antioxidant capacity of RMW, as demonstrated by the concentration-dependent increase in radical scavenging activity, is consistent with the findings of previous studies[34]. The particularly high scavenging rate in the ABTS assay suggested that RMW may contain compounds with high reducing power, which was a characteristic of many polyphenolic compounds[35]. This is further supported by the significant correlation between the total polyphenol content and

Table 3　DPPH, $ABTS^+$ and hydroxyl radicals scavenging activities of RMW

Concentration of RMW (mg/mL)	DPPH radical scavenging activity(%)	$ABTS^+$ radical scavenging activity(%)	Hydroxyl scavenging activity(%)
1.0	36.70±2.09^{f}	66.27±1.83^{e}	12.22±1.21^{d}
1.2	42.88±0.77^{e}	75.14±1.78^{d}	14.62±1.13^{d}
1.4	49.88±1.19^{d}	82.05±2.11^{c}	17.88±1.22^{c}
1.6	56.00±1.07^{c}	88.05±1.79^{b}	19.81±0.85^{bc}
1.8	61.77±1.37^{b}	94.65±0.33^{a}	21.95±0.81^{ab}
2.0	68.09±0.68^{a}	97.41±0.01^{a}	23.98±0.56^{a}

Note: Values followed by different letters within the same columns are significantly different (P<0.05).

antioxidant activity observed in this study. These results suggested that these extracts of RMW play a crucial role in its antioxidant properties.

2.7　Identification and Analysis of Compounds in RMW

Metabolite profiling of RMW identified 1078 and 178 distinct molecular species in positive and negative ionization modes (Figure 4). The analysis revealed several classes of bioactive compounds with established anti-diabetic properties, including flavonoids such as quercetin and kaempferol derivatives, which are known to enhance cellular glucose uptake through AMPK pathway activation and improve insulin sensitivity via modulation of IRS-1 phosphorylation[36−37]. Phenolic acids including chlorogenic acid and gallic acid were also detected, suggesting potential α-glucosidase inhibitory activity that may delay intestinal carbohydrate absorption[38]. Of particular significance was the identification of 1-DNJ, a potent α-glucosidase inhibitor clinically demonstrated to reduce postprandial hyperglycemia in a dose-dependent manner[39].

Pathway analysis demonstrated statistically significant enrichment (P<0.01) in several diabetes-relevant metabolic pathways. Glycolipid metabolism accounted for 38% of observed metabolite variance (P=2.3×10^{-5}). The Warburg Effect pathway showed particularly strong enrichment (P=4.1×10^{-4}), suggesting potential modulation of cellular energy metabolism through AMPK-mediated mechanisms like metformin, including mitochondrial complex I inhibition[40−41]. Significant enrichment was also observed in

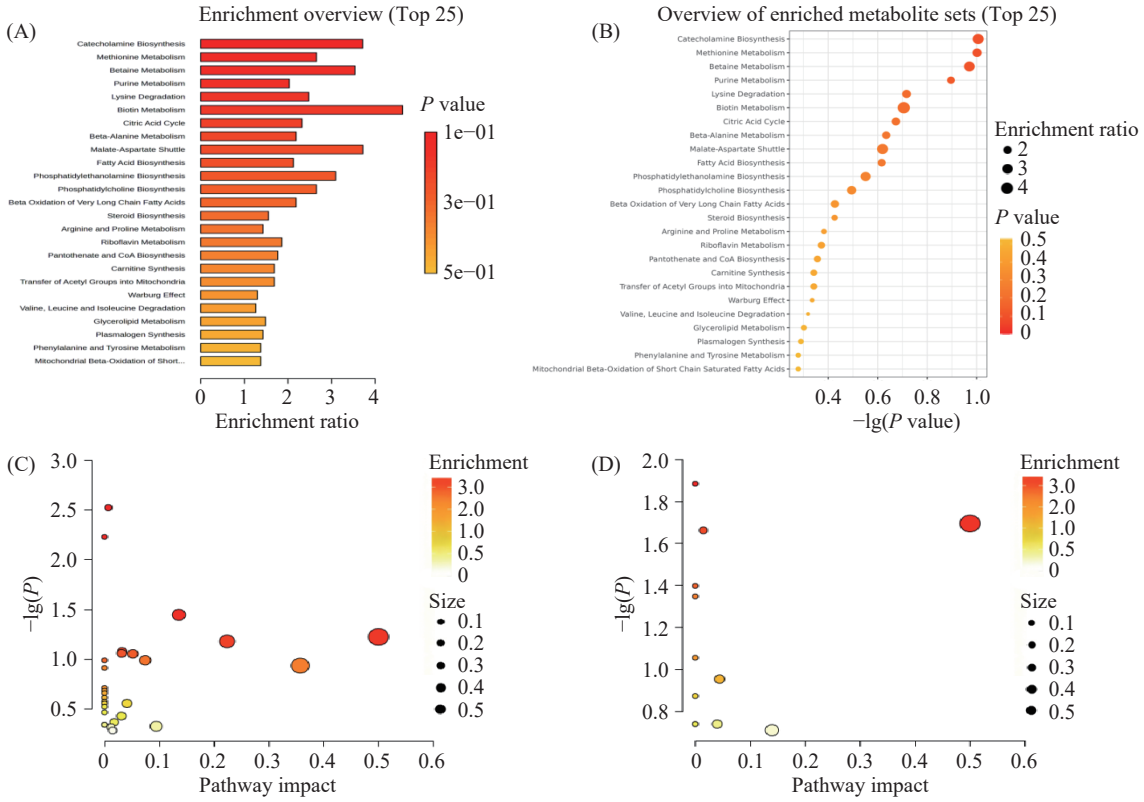


Fig.4　LC-MS/MS positive and negative ion

Note: (A) Histogram of enrichment analysis in positive ion model of RMW; (B) Bubble diagram of enrichment analysis in RMW negative ion model; (C) Bubble diagram of channel analysis in RMW positive ion mode; (D) Bubble diagram of channel analysis in RMW negative ion mode.

plasmalogen synthesis pathways (enrichment ratio= 5.2, P=0.003), consistent with emerging evidence of their critical role in β-cell function and insulin secretion[42−43].

The metabolic profile suggested multiple potential anti-diabetic mechanisms: a. PPAR-γ activation might promote insulin sensitivity through adipocyte differentiation and GLUT4 translocation. b. α-glucosidase inhibition could attenuate postprandial glucose excursions by delaying carbohydrate digestion. c. antioxidant components might preserve β-cell function by mitigating oxidative stress. This metabolic signature, characterized by diverse compounds targeting key diabetes-related pathways, positions RMW as a promising multi-target therapeutic agent.

2.8 RMW can prevent or inhibit the increase of body weight and blood glucose in mice

The animal experiments systematically confirmed RMW's multi-target therapeutic actions predicted by network pharmacology, demonstrating coordinated improvements across key metabolic parameters. Specifically, RMW treatment significantly attenuated HFD-induced weight gain (P<0.05 versus HD group), improved glucose tolerance (22.7% OGTT AUC reduction, P<0.01), enhanced insulin sensitivity (1.82±0.11 vs 1.23±0.09 ng/mL, P<0.01), and normalized HbA1c levels (5.2%±0.3% vs 6.8%±0.4%, P<0.01). These effects correlated with the pathway enrichment patterns identified in metabolite profiling.

The experimental results demonstrate RMW's multi-target anti-diabetic effects through three validated mechanisms: (a) lipid metabolism regulation via AMPK activation, (b) glucose control through carbohydrate digestion inhibition, and (c) β-cell protection via oxidative stress reduction. These findings align with the known pharmacological properties of mulberry-derived compounds[44−45]. This integrated metabolic improvement aligns with the established paradigm where multi-target botanical interventions outperform single-pathway drugs in metabolic disorders, as evidenced by recent polypharmacology studies[46]. These results conclusively validate the network pharmacology predictions, demonstrating RMW's coordinated multi-target action on diabetic metabolic dysregulation.

2.9 RMW can reduce dyslipidemia in mice with HFD

Dyslipidemia was a key risk factor for metabolic syndrome and cardiovascular diseases[47]. Our experimental model successfully recapitulated this condition, with HD animals exhibiting characteristic lipid abnormalities including elevated TC (21.4%, P<0.05), TG (142%, P<0.01), and LDL-C (40.7%, P<0.01), coupled with reduced HDL-C (33.0%, P<0.05) compared to ND. RMW intervention effectively reversed these perturbations, producing significant reductions in TG (31.7%, P<0.05) and LDL-C (18.8%, P<0.05), while increasing HDL-C (19.5%, P<0.05).

These therapeutic effects aligned precisely with our network pharmacology predictions, particularly regarding PPARG as a central regulatory node (Figure 1(C)). Mechanistically, the lipid improvements involved: (a) PPAR-γ-mediated enhancement of lipoprotein lipase activity for TG clearance, (b) LXR-α/ABCA1-dependent promotion of reverse cholesterol transport for HDL-C elevation, and (c) potential LDL receptor upregulation facilitating LDL-C clearance[48−49]. The selective modulation of atherogenic lipids (TG/LDL-C) without affecting total cholesterol suggests pathway-specific regulation rather than global cholesterol synthesis inhibition.

Notably, these lipid-modulating effects complemented RMW's anti-hyperglycemic actions through AMPK and insulin signaling pathways (Figure 3(B)), collectively demonstrating its multi-target capacity against metabolic syndrome. While previous reports described general lipid-modifying properties of mulberry extracts[48−49], this study advances the field by: (a) establishing direct links to glucose metabolism pathways, (b) validating computationally predicted target-pathway relationships (Figure 5(I)~Figure 5(L)), and (c) demonstrating coordinated metabolic improvements through integrated omics approaches.

2.10 Effect of RMW on oxidative stress in mice with HFD

The experimental results demonstrated that the high-fat diet successfully induced significant oxidative stress and inflammatory responses in the animal model. Compared to the ND group, the HD group exhibited markedly reduced levels of key antioxidant enzymes, including GSH (39.4% decrease, P<0.05), GSH-Px (53.3% decrease, P<0.01), SOD (20.3% decrease, P<0.05), and CAT (30.8% decrease, P<0.05). Concurrently, significant elevations were observed in pro-inflammatory cytokines (IL-1β: 28.0% increase, P<0.05; TNF-α: 145.5% increase, P<0.01). Treatment with RMW effectively ameliorated these metabolic disturbances, restoring GSH-Px activity to 90.5% of normal levels (P<0.05 versus HD group) and bringing SOD and CAT activities

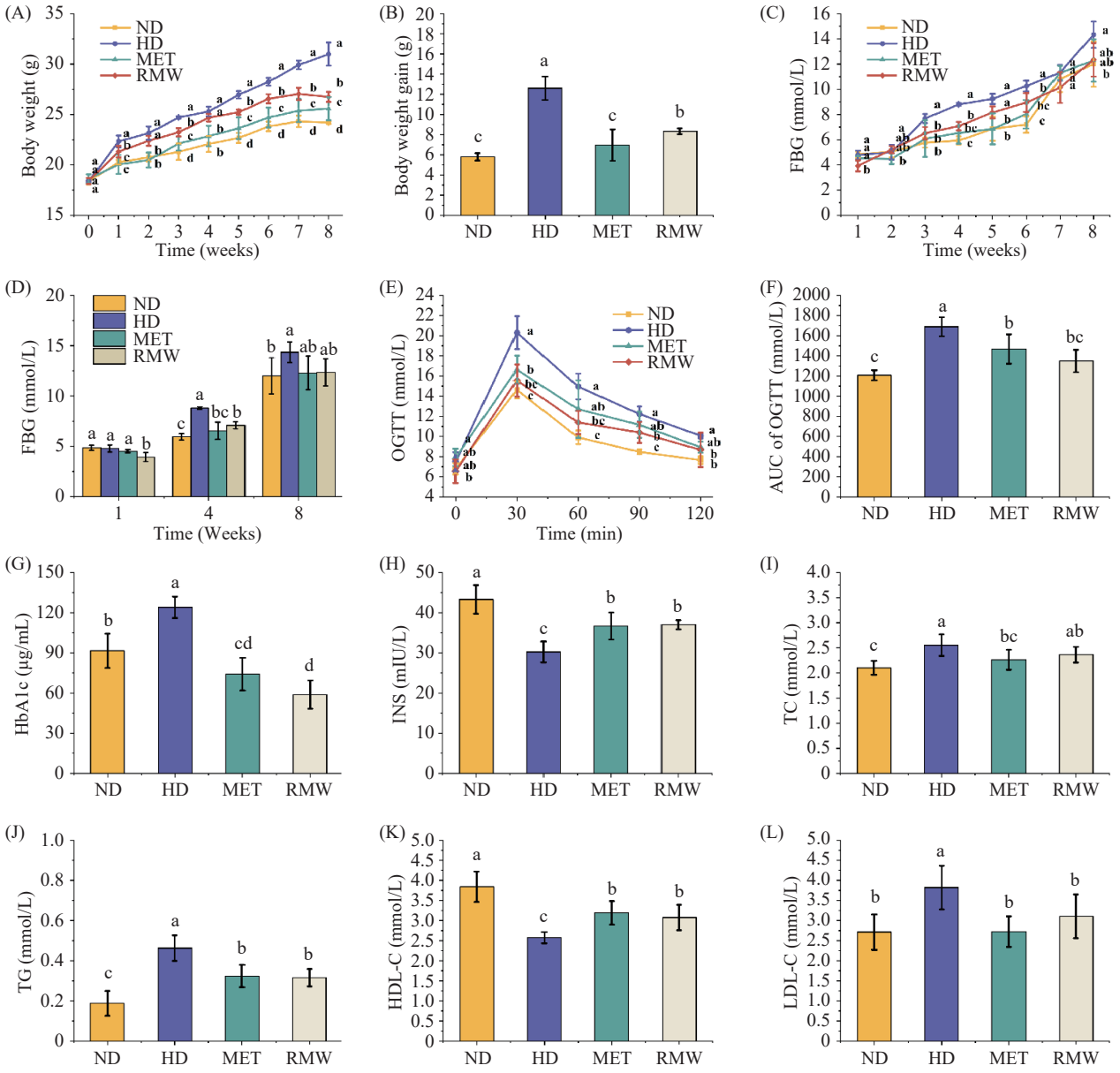


Fig.5　Effects of RMW on body weight and blood glucose in mice

Notes: (A)Body Weight; (B)Body Weight gain; (C)FBG: Fasting Blood Glucose; (D)FBG of 1 week, 4 weeks and 8 weeks; (E)OGTT; (F)AUC of OGTT; (G)HbA1c; (H)INS; (I)TC; (J)TG; (K)HDL-C; (L)LDL-C. In figures A, C and E, the different letter corner marks in the same column have significant differences (P<0.05). In other histogram, there were significant differences among groups with different letters (P<0.05).

back to near-normal ranges (P<0.05). After RM intervention, the levels of NO and MDA in the HD group were decreased, suggesting that RM may improve T2DM through antioxidation. The intervention also significantly attenuated inflammatory markers, reducing IL-1β by 20.7% and TNF-α by 11.7% (both P<0.05), with efficacy comparable to the MET positive control group (Figure 6).

These improvements were consistent with the network pharmacology predictions regarding Nrf2-mediated antioxidant responses and NF-κB pathway inhibition. The differential restorative effects on antioxidant enzymes (90.5% recovery of GSH-Px versus near-complete restoration of SOD/CAT) suggested a preferential enhancement of specific antioxidant systems by RMW. When combined with its anti-inflammatory actions, these findings highlighted RMW's multi-target therapeutic potential against metabolic dysregulation. Compared to previous reports on mulberry extracts[50−52], the current study provided more comprehensive mechanistic insights by: (a) quantitative demonstration of dose-dependent effects, (b) establishment of links to predicted pathways, and (c) simultaneous evaluation of oxidative and inflammatory markers. The concordance between computational predictions and experimental results substantiated the potential of RMW as a natural intervention for disorders

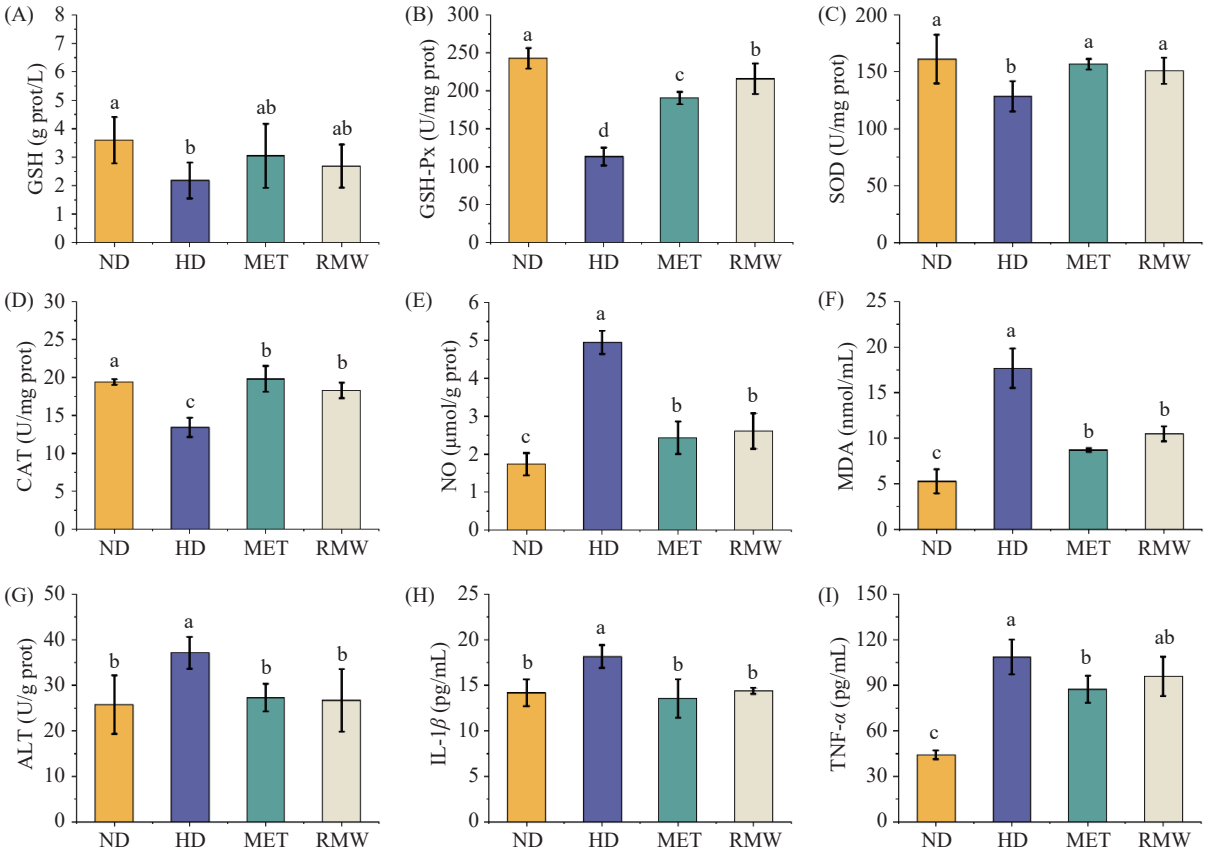


Fig.6 Effects of RMW on inflammatory factors and oxidative stress

Note: (A)GSH; (B)GSH-Px; (C)SOD; (D)CAT; (E)NO; (F)MDA; (G)ALT; (H)IL-1β; (I)TNF-α; There were significant differences among groups with different letters (P<0.05).

characterized by oxidative stress and chronic inflammation.

2.11 Effects of RMW on organ index and fat deposition

Organ and fat weights provided useful reference indicators for assessing metabolic changes and potential effects of interventions in diabetic mouse models[53]. As shown in Table 4, after the 8-week intervention, the liver index in the ND (4.00%±0.19%), MET (3.64%±0.11%) and RMW (3.77%±0.15%) groups were significantly lower than those in the HD group (4.48%±0.15%, P<0.05). While other organ indices remained unchanged (P>0.05), consistent with previous reports on mulberry polyphenols[54]. Notably, HD mice exhibited elevated epididymal WAT (2.30%±0.68% vs ND: 1.32%±0.53%, P<0.05) and mesenteric fat accumulation (1.40%±0.33% vs ND: 0.77%±0.14%, P<0.05)[55], confirming the metabolic disturbances characteristic of diabetic models. These tissue-specific effects correlated precisely with network pharmacology predictions, showing predominant activity in PPAR-γ and AMPK signaling pathways (Figure 1(C), Figure3(B)) that regulated hepatic and adipose tissue metabolism.

Table 4 Effects of RMW on organ and fat index in mice

Group	ND	HD	MET	RMW
Organ Index (%)				
Heart	0.52±0.04^a	0.50±0.06^a	0.52±0.05^a	0.47±0.02^a
Liver	4.00±0.19^b	4.48±0.15^a	3.64±0.11^c	3.77±0.15^c
Kidney	1.35±0.03^a	1.39±0.09^a	1.35±0.07^a	1.39±0.07^a
Splenic organ	0.23±0.02^a	0.25±0.02^a	0.22±0.02^a	0.24±0.02^a
Lung	0.56±0.07^a	0.53±0.03^a	0.51±0.04^a	0.58±0.04^a
Pancreas	0.11±0.07^a	0.08±0.02^a	0.09±0.04^a	0.07±0.03^a
Fat Index (%)				
Epididymal WAT	1.32±0.53^b	2.30±0.66^a	2.22±0.68^a	2.45±0.53^a
BAT	0.38±0.06^a	0.34±0.02^a	0.46±0.15^a	0.46±0.06^a
Renal fat	0.36±0.27^a	0.85±0.50^a	0.47±0.35^a	0.70±0.22^a
Mesenteric fat	0.77±0.14^b	1.40±0.33^a	1.11±0.23^a	1.18±0.28^a

Note: There were significant differences among groups with different letters (P<0.05).

The coordinated metabolic improvements align with established T2DM pathophysiology, demonstrated multi-target modulation through: (a) PPAR-γ-mediated insulin sensitization, (b) enhanced antioxidant defenses, and (c) attenuated inflammatory responses. The selective targeting of metabolic regulators (PPARG, INSR) and inflammatory mediators (IL6, TNF) explained the observed tissue specificity, while non-metabolic organs showed no significant changes (P>0.05). These findings supported RMW's potential as a targeted intervention for T2DM,

particularly for patients with concurrent metabolic dysfunction and hepatic steatosis, warranting further clinical investigation.

3 Conclusions

This study elucidated the multifaceted antidiabetic potential of RMW through integrated network pharmacology, metabolomics, and *in vivo* validation. Six major active compounds—cyanidin, quercetin, morin, and β-carotene—were screened from the 91 compounds identified in the TCMSP database. These compounds were predicted to interact with 158 potential targets, many of which were implicated in key diabetes-related signaling pathways, including MAPK, AGE–RAGE, FoxO, and insulin resistance pathways. Metabolomic profiling corroborated these findings by revealing enrichment in pathways associated with catecholamine biosynthesis, methionine metabolism, and lipid metabolism. In HFD-induced murine models, administration of RMW resulted in significant reductions in body weight and blood glucose levels, along with improvements in insulin sensitivity and lipid profiles. Additionally, RMW exhibited pronounced antioxidant and anti-inflammatory activities, as evidenced by increased DPPH and ABTS radical scavenging capacities, elevated antioxidant enzyme activities (GSH, GSH-Px, SOD, and CAT), and reduced expression of proinflammatory cytokines IL-1β and TNF-α. Collectively, these findings provide a novel theoretical basis for the treatment of diabetes. However, further studies employing cellular models are warranted to elucidate the precise molecular targets and signaling pathways modulated by RMW, thereby facilitating its future therapeutic development.

© The Author(s) 2026. This is an Open Access article distributed under the terms of the Creative Commons Attribution License (https://creativecommons.org/licenses/by-nc-nd/4.0/).

参考文献

[1] ElSAYED N A, ALEPPO G, ARODA V R, et al. Classification and diagnosis of diabetes: Standards of care in diabetes-2023[J]. Diabetes Care, 2023, 46(Suppl 1): S19−S40.

[2] de FRONZO R A, FERRANNINI E, GROOP L, et al. Type 2 diabetes mellitus[J]. Nature Reviews Disease Primers, 2015, 1: 15019.

[3] FEI Zhang, XU Yang, ZHANG Guoyu, et al. Natural products with potential hypoglycemic activity in T2DM: 2019-2023[J]. Phytochemistry, 2024, 223: 114130.

[4] CHO I H, CHENG R R, JUNG C W, et al. Effects of 1-Deoxynojirimycin on glycemic control: A systematic review and meta-analysis[J]. NFS Journal, 2025, 38: 100210.

[5] CHEN Xiaoxia, WU Junlin, FU Xiong, et al. Fructus *Mori polysaccharide* alleviates diabetic symptoms by regulating intestinal microbiota and intestinal barrier against TLR4/NF-κB pathway[J]. International Journal of Biological Macromolecules, 2023, 249: 126038.

[6] LEE J S, KIM Y R, SONG I G, et al. Cyanidin-3-glucoside isolated from mulberry fruit protects pancreatic β-cells against oxidative stress-induced apoptosis[J]. International Journal of Molecular Medicine, 2015, 35(2): 405−412.

[7] LOWN M, FULLER R, LIGHTOWLER H, et al. Mulberry-extract improves glucose tolerance and decreases insulin concentrations in normoglycaemic adults: Results of a randomised double-blind placebo-controlled study[J]. PLoS One, 2017, 12(2): e0172239.

[8] ZHANG Yue, LI Liang, CHAI Tao, et al. Mulberry leaf multi-components exert hypoglycemic effects through regulation of the PI-3K/Akt insulin signaling pathway in type 2 diabetic rats[J]. Journal of Ethnopharmacology, 2024, 319: 117307.

[9] ZHANG Yindi, LIU Junxi, WANG Feifei, et al. Mulberry leaf extract and deoxynojirimycin modulates glucose and lipid levels via the IRS1/PI3K/AKT signaling pathway in cells[J]. Journal of Food Biochemistry, 2025, 2025(1): 7345044.

[10] YUAN Zhongzhu, PAN Yingying, LENG Tian, et al. Progress and prospects of research ideas and methods in the network pharmacology of traditional Chinese medicine[J]. Journal of Pharmacy & Pharmaceutical Sciences, 2022, 25: 218−226.

[11] ZHAI Yiyan, LIU Liu, ZHANG Fanqin, et al. Network pharmacology: A crucial approach in traditional Chinese medicine research[J]. Chinese Medicine, 2025, 20(1): 8.

[12] YANG Songqin, ZHAO Mao, LU Mingxing, et al. Network pharmacology analysis, molecular docking integrated experimental verification reveal the mechanism of *Gynostemma pentaphyllum* in the treatment of type II diabetes by regulating the IRS1/PI3K/Akt signaling pathway[J]. Current Issues in Molecular Biology, 2024, 46(6): 5561−5581.

[13] DENG Yuru, CUI Jie, JIANG Yuxuan, et al. Exploring the nutraceutical potential of a food–medicine compound for metabolic-associated fatty liver disease *via* lipidomics and network pharmacology[J]. Foods, 2025, 14(7): 1257.

[14] WANG Guidan, DONG Jine. Network pharmacology approach to evaluate the therapeutic effects of mulberry leaf components for obesity[J]. Experimental and Therapeutic Medicine, 2022, 23(1): 56.

[15] NOGALES C, MAMDOUH Z M, LIST M, et al. Network pharmacology: Curing causal mechanisms instead of treating symptoms[J]. Trends in Pharmacological Sciences, 2022, 43(2): 136−150.

[16] LEE W Y, PARK K I, BAK S B, et al. Evaluating current status of network pharmacology for herbal medicine focusing on identifying mechanisms and therapeutic effects[J]. Journal of Advanced Research, 2025, 76: 799−815.

[17] XU Xinyi, LIU Leping, CAO Xueshuai, et al. Network pharmacology and molecular docking analysis on molecular targets and mechanism prediction of Huanglian Jiedu Decoction in the treatment of COVID-19[J]. Digital Chinese Medicine, 2022, 5(1): 18−32.

[18] QI Yanjiao, ZANG Rongxing, LU Huining, et al. Network

pharmacology and bioinformatics approach reveals the hypolipidemic mechanism of Dan Tian Jiang Zhi pill[J]. Medicinal Chemistry Research, 2020, 29(2): 243−254.

[19] XU Xue, ZHANG Wuxia, HUANG Chao, et al. A novel chemometric method for the prediction of human oral bioavailability[J]. International Journal of Molecular Sciences, 2012, 13(6): 6964−6982.

[20] YOU T H. Research on the antioxidant and anti-aging effects of mulberry polyphenolic compounds[D]. Guangdong: Guangdong Pharmaceutical University, 2015.

[21] ZHANG X Y. Study on the biological activity of lyophilized mulberry powder[D]. Changchun: Jilin University, 2019.

[22] WANG Risi, DONG Panhao, SHUAI Xixiang, et al. Evaluation of different black mulberry fruits (*Morus nigra* L.) based on phenolic compounds and antioxidant activity[J]. Foods, 2022, 11(9): 1252.

[23] VUKMIROVIĆ S, ILIĆ V, TADIĆ V, et al. Comprehensive analysis of antioxidant and hepatoprotective properties of *Morus nigra* L[J]. Antioxidants, 2023, 12(2): 382.

[24] CHEN Tao, SHUANG Feifan, FU Qingyue, et al. Evaluation of the chemical composition and antioxidant activity of mulberry (*Morus alba* L.) fruits from different varieties in China[J]. Molecules, 2022, 27(9): 2688.

[25] ZHANG L Y, QIN S H, TANG S N, et al. Qualitative analysis of multiple phytochemical compounds in tojapride based on UHPLC Q-exactive orbitrap mass spectrometry[J]. Molecules, 2022, 27(19): 6639.

[26] AVULA B, KATRAGUNTA K, OSMAN A G, et al. Advances in the chemistry, analysis and adulteration of anthocyanin rich-berries and fruits: 2000-2022[J]. Molecules, 2023, 28(2): 560.

[27] ZHAO Xianyang, REN Da, JIN Rui, et al. Development of UHPLC-Q-exactive orbitrap/MS technique for determination of proanthocyanidins (PAs) monomer composition content in persimmon[J]. Plants, 2024, 13(11): 1440.

[28] DUAN Yuhui, DAI Hongyu, AN Yongcheng, et al. Mulberry leaf flavonoids inhibit liver inflammation in type 2 diabetes rats by regulating TLR4/MyD88/NF-*κ*B signaling pathway[J]. Evidence-Based Complementary and Alternative Medicine, 2022, 2022 (1): 3354062.

[29] CHEN Chun, YOU Lijun, HUANG Qiang, et al. Modulation of gut microbiota by mulberry fruit polysaccharide treatment of obese diabetic db/db mice[J]. Food & Function, 2018, 9(7): 3732−3742.

[30] WINZELL M S, AHRÉN B. The high-fat diet-fed mouse: A model for studying mechanisms and treatment of impaired glucose tolerance and type 2 diabetes[J]. Diabetes, 2004, 53(Suppl 3): S215-S219.

[31] RAMAPPA V K, SRIVASTAVA D, SINGH P, et al. Mulberries: A promising fruit for phytochemicals, nutraceuticals, and biological activities[J]. International Journal of Fruit Science, 2020, 20(sup3): S1254−S1279.

[32] SURIYAPROM S, KAEWKOD T, PROMPUTTHA I, et al. Evaluation of antioxidant and antibacterial activities of white mulberry (*Morus alba* L.) fruit extracts[J]. Plants, 2021, 10(12): 2736.

[33] MOHAMMED A S A, NAVEED M, JOST N. Polysaccharides; classification, chemical properties, and future perspective applications in fields of pharmacology and biological medicine (a review of current applications and upcoming potentialities)[J]. Journal of Polymers and the Environment, 2021, 29(8): 2359−2371.

[34] LALHMINGHLUI K, JAGETIA G C. Evaluation of the free-radical scavenging and antioxidant activities of chilauni, *Schima wallichii* korth *in vitro*[J]. Future Science OA, 2018, 4(2): FSO272.

[35] FLOEGEL A, KIM D O, CHUNG S J, et al. Comparison of ABTS/DPPH assays to measure antioxidant capacity in popular antioxidant-rich US foods[J]. Journal of Food Composition and Analysis, 2011, 24(7): 1043−1048.

[36] HUANG Qun, CHEN Lei, TENG Hui, et al. Phenolic compounds ameliorate the glucose uptake in HepG2 cells' insulin resistance *via* activating AMPK Anti-diabetic effect of phenolic compounds in HepG2 cells[J]. Journal of Functional Foods, 2015, 19: 487−494.

[37] ALI M, HASSAN M, ANSARI S A, et al. Quercetin and kaempferol as multi-targeting antidiabetic agents against mouse model of chemically induced type 2 diabetes[J]. Pharmaceuticals, 2024, 17(6): 757.

[38] ALEIXANDRE A, GIL J V, SINEIRO J, et al. Understanding phenolic acids inhibition of *α*-amylase and *α*-glucosidase and influence of reaction conditions[J]. Food Chemistry, 2022, 372: 131231.

[39] FONGSODSRI K, THAIPITAKWONG T, RUJIMONGKON K, et al. Mulberry-derived 1-deoxynojirimycin prevents type 2 diabetes mellitus progression *via* modulation of retinol-binding protein 4 and haptoglobin[J]. Nutrients, 2022, 14(21): 4538.

[40] ITO M, GURUMANI M Z, MERSCHER S, et al. Glucose- and non-glucose-induced mitochondrial dysfunction in diabetic kidney disease[J]. Biomolecules, 2022, 12(3): 351.

[41] GUO Sijia, ZHANG Chenhao, ZENG Haiou, et al. Glycolysis maintains AMPK activation in sorafenib-induced Warburg effect[J]. Molecular Metabolism, 2023, 77: 101796.

[42] HONSHO M, FUJIKI Y. Regulation of plasmalogen biosynthesis in mammalian cells and tissues[J]. Brain Research Bulletin, 2023, 194: 118−123.

[43] CHEN Y, CRUZAT V F, NEWSHOLME P. Chapter 3 - *β*-Cell Metabolism, Insulin Production and Secretion: Metabolic Failure Resulting in Diabetes[M]//Mauricio D. Molecular Nutrition and Diabetes. San Diego, Academic Press. 2016: 29−40.

[44] ZHANG Ruiyuan, ZHANG Qian, ZHU Shun, et al. Mulberry leaf (*Morus alba* L.): A review of its potential influences in mechanisms of action on metabolic diseases[J]. Pharmacological Research, 2022, 175: 106029.

[45] THAIPITAKWONG T, NUMHOM S, ARAMWIT P. Mulberry leaves and their potential effects against cardiometabolic risks: A review of chemical compositions, biological properties and clinical efficacy[J]. Pharmaceutical Biology, 2018, 56(1): 109−118.

[46] WANG Ying, HU Baichun, FENG Shasha, et al. Target recognition and network pharmacology for revealing anti-diabetes mechanisms of natural product[J]. Journal of Computational Science, 2020, 45: 101186.

[47] ISLAM M S, WEI Ping, SUZAUDDULA M, et al. The interplay of factors in metabolic syndrome: Understanding its roots and complexity[J]. Molecular Medicine, 2024, 30(1): 279.

[48] LEE S, LEE M S, CHANG E, et al. Mulberry fruit extract

promotes serum HDL-cholesterol levels and suppresses hepatic microRNA-33 expression in rats fed high cholesterol/cholic acid diet[J]. Nutrients, 2020, 12(5): 1499.

[49] CHAIWONG S, CHATTURONG U, CHANASONG R, et al. Dried mulberry fruit ameliorates cardiovascular and liver histopathological changes in high-fat diet-induced hyperlipidemic mice[J]. Journal of Traditional and Complementary Medicine, 2021, 11(4): 356−368.

[50] MYSZKO M, BYCHOWSKI J, SKRZYDLEWSKA E, et al. The dual role of oxidative stress in atherosclerosis and coronary artery disease: Pathological mechanisms and diagnostic potential[J]. Antioxidants, 2025, 14(3): 275.

[51] TAN B L, NORHAIZAN M E. Effect of high-fat diets on oxidative stress, cellular inflammatory response and cognitive function[J]. Nutrients, 2019, 11(11): 2579.

[52] WANG Zichao, WANG Zhe, HUANG Wenhui, et al. Antioxidant and anti-inflammatory activities of an anti-diabetic polysaccharide extracted from *Gynostemma pentaphyllum* herb[J]. International Journal of Biological Macromolecules, 2020, 145: 484−491.

[53] WANG C Y, LIAO J K. A mouse model of diet-induced obesity and insulin resistance[J]. Methods in Molecular Biology, 2012, 821: 421−433.

[54] LI Rui, ZHU Qubo, WANG Xiaoyan, et al. Mulberry leaf polyphenols alleviated high-fat diet-induced obesity in mice[J]. Frontiers in Nutrition, 2022, 9: 979058.

[55] KALAPUR S, SINGH C. Correlation of visceral adiposity index with visceral fat in obese patients with and without Type 2 diabetes mellitus[J]. J Assoc Physicians India, 2022, 70(4): 11−12.